Combined effects of aquaporin-4 and hypoxia produce age-related hydrocephalus

José Luis Trillo-Contreras[1,2], Reposo Ramírez-Lorca[1,2], Laura Hiraldo-González[1,2], Ismael Sánchez-Gomar[1], Ana Galán-Cobo[1], Nela Suárez-Luna[1,2], Eva Sánchez de Rojas-de Pedro[1], Juan José Toledo-Aral[1,2,3], Javier Villadiego[1,2,3#] and Miriam Echevarría[1,2,#]

1. Institute of Biomedicine of Seville (IBiS), Virgen del Rocío University Hospital. (HUVR)/Spanish National Research Council (CSIC)/University of Seville, Seville, 41013, Spain.
2. Department of Physiology and Biophysics, University of Seville, Seville, 41009, Spain.
3. Network Center for Biomedical Research in Neurodegenerative Diseases (CIBERNED), Spain.

#Address correspondence to Dr. Miriam Echevarría (irusta@us.es) or Dr. Javier Villadiego (fvilladiego@us.es), Instituto de Biomedicina de Sevilla-IBiS, Avda. Manuel Siurot s/n, 41013 Sevilla, Spain. Tel: (+34) 955923036; Fax: (+34) 955923101.

ABSTRACT

AQP4, present in ependymal cells, in glia limitans and abundantly in pericapillary astrocyte foot processes, and AQP1, expressed in choroid plexus epithelial cells, are believed to play an important role in cerebrospinal fluid (CSF) production and may be involved in the pathophysiology of age-dependent hydrocephalus. The finding that brain AQP expression is regulated by low oxygen tension led us to investigate how hypoxia and elevated levels of cerebral AQPs may result in an increase in CSF production that could be associated with a hydrocephalic condition. Here we have explored, in young and aged mice exposed to hypoxia, whether AQP4 and AQP1 participate in the development of age-related hydrocephalus. Choroid plexus, striatum, cortex and ependymal tissue were analyzed separately both for mRNA and protein levels of AQPs. In addition, parameters such as total ventricular volume, intraventricular pressure, CSF outflow rate, ventricular compliance and cognitive function were studied in wt, AQP1$^{-/-}$ and AQP4$^{-/-}$ live animals subjected to hypoxia or normoxia. Our data demonstrate that hypoxia is involved in the development of age-related hydrocephalus by a process that depends on AQP4 channels as a main route for CSF movement. Significant increases in AQP4 expression that occur over the course of animal aging, together with a reduced CSF outflow rate and ventricular compliance, contribute to produce more severe hydrocephalus related to hypoxic events in aged mice, with a notable impairment in cognitive function. These results indicate that physiological events and/or pathological conditions presenting with cerebral hypoxia/ischemia contribute to the development of chronic adult hydrocephalus.

1. INTRODUCTION

Cerebrospinal fluid (CSF) is the main component of the extracellular fluid in the central nervous system (CNS) [1-6]. Apart from its important protective function cushioning the brain and spinal cord against mechanical injury, this fluid represents an important pathway for clearance of waste from neural tissue, and to some extent the delivery of nutrients, hormones and gases [7]. CSF directly communicates with brain interstitial fluid (IF), and in doing so, plays an important role in maintaining the homeostasis of the external fluid bathing glia and neurons. Regulation of brain fluid content (ions and all other solutes) and volume is critical for the normal functioning of the CNS, which is highly sensitive to changes in the osmolarity and hydrostatic pressures of CSF and IF. In a normal stationary state, there must be an equilibrium between the rates of CSF production and absorption in order to avoid conditions that may trigger hydrocephalus and even parenchymal edema.

It has been suggested that brain aquaporins (AQPs), particularly AQP4 and AQP1, play an important role in CSF homeostasis, and a simplistic view of their functions associates AQP1 with CSF secretion and AQP4 with its absorption [8-11]. Their distribution, with AQP1 expressed in epithelial cells of the choroid plexus [12-15] and AQP4 present in ependymal cells bordering the intraventricular compartments and glia limitans and particularly abundant in pericapillary astrocyte foot processes [8, 10, 16], provides arguments to propose that both proteins take part in the homeostasis of CSF.

Nevertheless, AQP water permeability is associated with general fluid movement among the different brain compartments, namely, blood, CSF and IF, but can also be expected to participate in the pathophysiology of brain fluid disorders. Alterations in the expression of these proteins are associated with the development of brain edema and hydrocephalus. In AQP1-null mice, the lack of AQP1 was associated with a potential beneficial effect on edema produced by a cerebral lesion [14], and kaolin-induced hydrocephalus [17]. Likewise, other studies have suggested an important role for AQP4 in animal models of edema and hydrocephalus [8, 18-23]. Specifically, for instance, AQP4 participates in the clearance of extracellular brain fluid toward the paravascular space in interstitial edema [24, 25]. Further, higher AQP4

expression was observed at the blood-brain barrier (BBB) and blood-CSF interfaces in pharmacologically-induced models of hydrocephalus [24, 26]. Moreover, AQP4$^{-/-}$ mice, developed greater ventriculomegaly and higher intracranial pressure (ICP) after kaolin injection, suggesting an adaptive role of AQP4 to resolve the hydrocephalic situation [27].

Idiopathic normal pressure hydrocephalus (iNPH), also commonly called chronic adult hydrocephalus, is a neurological disorder associated with ageing characterized by ventriculomegaly and cognitive deficits [28]. Although alterations in CSF production, movement or drainage have been linked with this disorder, the pathophysiological mechanisms underlying this disease are unknown. Apart from the body of evidence that suggests an involvement of cerebral AQPs in CSF homeostasis and hydrocephalus, hypoxia has also been associated with the pathophysiology of iNPH [29, 30]. In this context, the findings that cerebral AQP expression is altered by hypoxic or ischemic conditions [31-34] and by aging [35], allow us to study how possible modifications of cerebral AQP expression produced by these conditions could alter CSF homeostasis causing or aggravating hydrocephalus.

In the present study, we analyzed changes in the expression of brain AQPs in young and aged animals upon hypoxic treatment. We relate such changes to parameters such as total ventricular volume measured by magnetic resonance imaging (MRI), and intraventricular pressure (IVP), CSF outflow rate and ventricular compliance measured by intraventricular recordings in live animals. Here, we demonstrate that hypoxia produces a hydrocephalic condition that could even develop into a considerably more severe hydrocephalus in aged animals, in which upregulation of AQP4 expression is critically involved. An interesting translational finding of our work is that aged mice exposed to chronic hypoxia reproduce the main symptoms of iNPH [36, 37], namely, larger ventricles, a slightly elevated intracranial pressure, decreased CSF outflow and ventricular compliance, as well as cognitive deficits. Therefore, chronic hypoxic aged mice appear to be an excellent animal model for studying the pathophysiology, potential diagnostic biomarkers and new treatments for chronic hydrocephalus in adults.

2. MATERIAL AND METHODS

2.1. Animal care and hypoxic treatments

C57BL/6 mice (Charles River), AQP1$^{-/-}$, AQP4$^{-/-}$ (kindly provided by Dr. A. Verkman, UCSF, CA) and wildtype (wt) littermates were housed at a controlled temperature (22±1ºC) in a 12 h light/dark cycle, with *ad libitum* access to food and water. AQP1$^{-/-}$ and AQP4$^{-/-}$ mice were outcrossed for at least eight generations to obtain a C57BL/6 genetic background. For all experiments, mice were considered young at 2-4 months old, and aged at >14 months old. The AQP1$^{-/-}$ and AQP4$^{-/-}$ mice were genotyped as indicated previously for AQP1 [38] and for AQP4 [38]. Mice were maintained either in normal conditions (normoxia) or exposed to hypoxia (48 hours or 5 days at 10% O_2) using an hermetically sealed chamber (Coy Laboratory Products, Inc., Grass Lake, MI) with continuous monitoring and control of gas concentrations, temperature and humidity as previously described [39].

The mice were sacrificed under anesthesia with a combination of 100 mg/kg ketamine (Pfizer) and 10 mg/kg xylazine (Bayer). All experiments were performed in accordance with the European Directive 2010/63/EU and the Spanish RD/53/2013 on the protection of animals used for scientific purposes. The study was approved by the Animal Research Committee of Virgen del Rocío University Hospital (26/01/2017/017; University of Seville).

2.2. RNA extraction and quantitative reverse transcription PCR analysis

Cortex and striatum total RNA were isolated using TRIzol reagent (Invitrogen) following the manufacturer's protocol. For tissues with small amounts of sample (choroid plexus and ependymal tissue bordering the lateral and third ventricle), pools of three animals were used, and the total RNA was isolated using the RNeasy Micro Kit (Qiagen). RNA was only pre-amplified, with an Ambion® WT Expression Kit (Invitrogen), in experiments where too little starting tissue was available, such as those performed with total RNA from old animals, and in the young animals used as their controls. Quantity and purity of RNA were assessed with a NanoDrop ND-1000 UV–vis spectrophotometer (Thermo Fisher), and cDNA synthesis was performed using SuperScript II RNase H$^-$ reverse transcriptase kits (Invitrogen). Relative mRNA expression levels of the genes studied were quantified using quantitative real-time polymerase chain

reaction (PCR) analysis with the ABI PRISM 7500 Sequence Detection System (Applied-Biosystems), SYBR Green PCR Master mix (Applied-Biosystems) and the thermocycler conditions recommended by the manufacturer. Amplification of 18S ribosomal RNA was determined and used to normalize expression levels to compensate for variation in RNA input amounts. Primers were designed using the Primer Express software v2.0 (Applied Biosystems) and its sequences are indicated in the supplementary material (Supplementary Material-1). All samples were analyzed in triplicate.

2.3. Histological analyses

Following normoxia or hypoxia treatments, animals were intracardially perfused with 50 ml of 4% paraformaldehyde dissolved in PBS (Sigma). Brains were immediately extracted and processed for cryostat cutting as previously described [39, 40]. Coronal sections (30-µm thick) were cut in a cryostat (Leica). Glial fibrillary acid protein (GFAP), AQP1 or AQP4 immunofluorescence was performed as previously described [41] using respectively monoclonal anti-GFAP (1:300; Sigma), polyclonal AQP1 (1:500; Abcam) and polyclonal AQP4 (1:100; α-Diagnostic). Anti-mouse IgG conjugated with Alexa Fluor488 or anti-rabbit IgG conjugated with Alexa Fluor568 (1:400; Invitrogen) were used as secondary antibodies. Nuclei were stained with DAPI (1:1000; Sigma). Tissue sections were mounted with Dako fluorescence mounting medium (Dako). Confocal images were acquired using a Nikon A1R$^+$ confocal microscope.

Optical density (OD) analysis was performed, for a total of five sections from each animal, covering the parietal cortex. The OD was measured from digitized images using the NIH Image software (ImageJ; NIH) as previously described [42, 43].

2.4. Western blot analysis

Tissues were dissected from animals and frozen in liquid N_2 for protein extraction. Samples were homogenized in lysis buffer containing 50 mM HEPES, pH 7.3, 250 mM NaCl, 5 mM EDTA, 0.2% (v/v) NP-40, 5 mM dithiothreitol and 1% (v/v) of a cocktail of protease inhibitors (Sigma) and were left on ice for 5 min. After centrifugation at 16000 g for 15 min at 4ºC, the supernatants were recovered. Lysates were loaded and resolved on 10% SDS-

polyacrylamide gel electrophoresis followed by transfer to a polyvinylidene fluoride membrane (Hybond-P; GE Healthcare, Piscataway, NJ). Membranes were probed with 1:1000 anti-AQP1 (Abcam), 1:250 anti-AQP4 (α-Diagnostic) or 1:10000 anti-beta Actin (Abcam) antibodies, developed with the ECL Plus Western Blotting Detection System (GE Healthcare) and visualized using a Typhoon 9400 imager (Amersham Biosciences).

2.5. Magnetic resonance imaging

Magnetic resonance images were taken to assess ventricle sizes as an indirect indicator of CSF production. Mice were anesthetized using 0.5-2.5% sevoflurane with spontaneous breathing. The studies were performed using an ICON 1 Tesla system (Bruker), with a mouse body radiofrequency coil, at the animal facilities of the institute (IBiS). Ventricular volumes were estimated from T2-weighted 3D rapid acquisition with relaxation enhancement sequences of coronal brain sections (repetition time, 95 ms; echo time, 3250 ms; plane resolution, 0.188 x 0.188 x 0.563 mm; thickness, 0.5 mm; rare factor, 8; and 32 slices). All the images were analyzed with VIRTUE software (Diagnosoft) and ImageJ 1.45 software (Wayne Rasband, National Institute of Health).

2.6. Intraventricular pressure measurements

The IVP was measured using a fluid-filled 34-gauge micropipette (Hamilton) inserted into the lateral ventricle through the cerebral cortex as previously described [14]. The micropipette was connected using noncompliant tubing to a pressure transducer (TSD104A; Biopac Systems) interfaced to a recording system (model MP150; Biopac Systems). The circuit also permits artificial CSF (aCSF) infusion by a syringe pump (KD Scientific). Briefly, mice were anesthetized with 100 mg/kg ketamine (Pfizer) and 10 mg/kg xylazine (Bayer) and immobilized, in prone position, in a stereotaxic device (Stoelting). A micropipette, with an aCSF infusion rate of 0.3 µl/min, was placed in the parietal cortex above the lateral ventricle (from bregma in mm: anteroposterior, -0.2; lateral, +1.0; and ventral, -1.0). Once the pipette enters the brain parenchyma, the pressure gradually increases and when the pressure was >40 cm H_2O, the infusion was stopped and the pipette was slowly advanced. The pressure dropped promptly when the pipette tip reached the lateral ventricle (see Fig.

2C). Then, IVP was continuously monitored and recorded.

2.7. Systemic blood pressures measurements

The mean arterial blood pressure, systolic and diastolic blood pressures were monitored by using a blood pressure analysis system for mouse (BP-2000 Series II; Visitech Systems – Physiological Research Instruments).

2.8. Cerebrospinal fluid outflow dynamics and ventricular compliance measurements

CSF outflow dynamics were measured by the constant-rate infusion method reported by Oshio et al. [14]. Briefly, a micropipette was located in the lateral ventricle as described before, and IVP was recorded during continuous infusion of a CSF into the lateral ventricle at rates of 0.5, 1.5, 3, 7 and 14 µl/min. Each infusion rate was maintained until a steady-state IVP was recorded, resulting in a step-wise increase in IVP (see Fig. 4A). The CSF outflow resistance was obtained by linear regression from the infusion rate and IVP. Ventricular compliance was measured by calculating the increase in IVP produced by the infusion of 1.75 µl of aCSF (into the lateral ventricle at rate of 14 µl/min).

2.9. Novel object recognition testing

Novel object recognition tests were performed in accordance with previously described methods [44]. As indicated in Figure 3D, a novel object recognition test was performed after the hypoxic treatment (5 days at 10% O2). Before start the behavioral test, mice were left for 10 minutes exploring the box (50 x 50 x 40 cm). Then, during the sample trial, mice were placed into the arena with two identical objects and the behavior of the animal was video recorded from a suspended camera. After 10 minutes, the animal was removed from the arena and placed back into the home cage and the arena was cleaned. After 3 hours, the novel object trial was performed. Mice were tested again in the same arena, but with one of the two familiar items randomly replaced with a novel object (with similar discrimination index), and video recorded again for 10 minutes. The object interactions were analyzed using the Novel Object Recognition Biobserve software (Biobserve GmbH).

2.10. Statistical analysis

Each experimental group consisted of 3-12 mice; the specific numbers (n) are shown in each figure. Data are presented as mean±standard error of the mean (SEM), and the statistical test used is indicated in each figure legend. In all cases, the data were tested for normality (Kolmogorov-Smirnov test) and equal variance. When these properties were confirmed, analysis of variance was carried out with Bonferroni post hoc analysis for multiple group comparisons, or Student's t-test (for two-group comparisons); otherwise, the non-parametric Kruskal–Wallis H test (for multiple comparisons) or Mann–Whitney U test (for-two group comparisons) were used. All statistical analyses were conducted using IBM SPSS Statistics for Windows, Version 20.

3. RESULTS

3.1. Cerebral AQP expression changes in the brain of young mice exposed to hypoxia.

Levels of AQP expression in choroid plexus, striatum, cortex and ventricular lining tissue from young wt mice were analyzed after 48 hours of hypoxia (10% O_2) and after chronic hypoxic treatment (5 days at 10% O_2) and compared to levels observed under normoxic conditions. Expression of AQP1 was only detected in the choroid plexus of young wt animals as previously indicated [10, 12]. Although AQP1 mRNA and protein levels were slightly higher after 48 hours of hypoxia no significant differences with respect to normoxia were found after any of the hypoxia treatments analyzed (Fig. 1A, B and Supp. Mat. 2). Levels of AQP1 detected in all other brain tissues studies were negligible, as indicated previously elsewhere [9]. In contrast, AQP4 was widely expressed in tissues including the cortex, striatum and ependymal tissue bordering the lateral and third ventricles (Fig 1 and Supp. Mat. 2).

Quantification of AQP4 mRNA levels in the choroid plexus (Fig 1A) indicated a significant increase in expression after 48 hours of hypoxia that correlates with the appearance of AQP4 protein in the choroid plexus after the hypoxic treatments (Fig. 1B). In the cortex, a transient induction of AQP4 protein was detected after 48 hours of hypoxia (Fig. 1C,D and Supp. Mat. 2A) and this can be attributed to the previously described overexpression of AQP4 mRNA in cortical astrocytes after 8 hours of hypoxia [45].

On the other hand, after chronic hypoxia (5 days), cortical AQP4 protein levels were lower again (Fig. 1C,D). Such a reduction in AQP4 protein levels could be related to the decrease in the AQP4 mRNA observed after 48 hours of hypoxia (Fig. 1A). A detailed analysis of AQP4 expression in the cortex showed, as previously found by single-cell RNA sequencing [46], that cortical AQP4 expression is mainly associated with astrocytes in the outer layers that have high expression of glial fibrillary acid protein ($GFAP^{high}$).

3.2. Chronic hypoxia induces slight enlargement of ventricles depending on the presence of AQP4.

In order to study how hypoxia might participate in the onset of hydrocephalus, brain ventricle size was compared in wt, $AQP1^{-/-}$ and $AQP4^{-/-}$ young mice

maintained in normoxia or chronic hypoxia (10% O_2 for 5 days). Ventricle size was estimated from MRI images of coronal brain sections (Fig. 2A). As shown in Figure 2B, chronic hypoxia was associated with a slight increase in the total ventricular volume of both wt and AQP1$^{-/-}$ mice. In the case of AQP1$^{-/-}$ mice, which had slightly lower ventricular volumes in normoxia, the increase in volume upon hypoxia treatment led to ventricular volumes similar to those observed in the wt hypoxic animals. In contrast, no differences were observed in the total ventricular volume of AQP4$^{-/-}$ mice exposed to hypoxia compared to those maintained in normoxia, indicating a key role for AQP4 in the loading of ventricles with CSF that occurs due to hypoxia exposure.

We then measured the effect of chronic hypoxia on the IVP of wt, AQP1$^{-/-}$ and AQP4$^{-/-}$ young mice (Figure 2C,D). As previously described [14], a significant lower IVP was detected in the AQP1$^{-/-}$ mice with respect to the wt mice (4.92±0.7 and 4.39±0.8 cm H_2O for the AQP1$^{-/-}$ mice in normoxia and hypoxia; vs 7.90±0.5 and 7.71±1.1 cm H_2O for wt mice in normoxia and hypoxia, respectively; $p<0.05$; Figure 2D). Intermediate IVP values were obtained in the AQP4$^{-/-}$ mice (6.21±1.0 and 6.03±0.8 cm H_2O in normoxia and hypoxia, respectively), indicating a slight reduction (~20%) with respect to the wt mice. Interestingly, as shown in Figure 2D, hypoxic treatment was not associated with changes in IVP in any of the groups (wt, AQP1$^{-/-}$ or AQP4$^{-/-}$ mice), indicating that the slight increases in ventricular volume produced by hypoxia in the wt and AQP1$^{-/-}$ mice were not accompanied by variations in IVP. In addition, because CSF is produced by modification of blood plasma, and in order to analyze if the changes observed in the ventricular volume or IVP might be due to alterations in systemic arterial blood pressure caused by the hypoxia and/or the absence of AQPs, arterial blood pressure was monitored in all of the experimental conditions and no differences were found between groups (Supplementary Material 3A).

3.3. Chronic hypoxia produces hydrocephalus in aged mice depending on the presence of AQP4.

We studied how chronic hypoxia affects ventricular volume in aged mice (≥14 months old). As shown in Figure 3A,B, MRI of coronal brain sections revealed a large increase in the ventricular volume in aged wt and AQP1$^{-/-}$ mice subjected

to chronic hypoxia (5 days, 10% O_2). The quantitative analysis of ventricular volume confirmed the larger ventricle size in hypoxic aged wt and AQP1$^{-/-}$ animals (>44% larger than in normoxic controls in both cases), and this was markedly larger than the volume observed in young wt animals exposed to hypoxia (~15% larger than in normoxic controls). Notably, the absence of AQP4 completely abolished the hypoxic ventricle enlargement in aged mice (Fig. 3B). Unlike what occurred in young animals, in aged wt and AQP1$^{-/-}$ mice, exposure to hypoxia produced a moderate but statistically significant increase in IVP (Fig. 3C). In accordance with the MRI data, the lack of AQP4 also blocked the increase in IVP observed in aged wt and AQP1$^{-/-}$ mice (Fig. 3C). Again, the changes observed both in the ventricular volume and IVP in the different experimental groups of aged mice cannot be attributed to modifications in the systemic arterial blood pressure (Supplementary Material 3B).

Given the similar response shown by the wt and AQP1$^{-/-}$ mice in all measurements performed up to this point and since the analysis of the ventricle volume and IVP clearly indicate that the ventricle CSF overload produced by hypoxia is mediated by AQP4, in the subsequent experiments we only analyzed wt vs AQP4$^{-/-}$ mice.

Next, we studied, in wt and AQP4$^{-/-}$ mice, whether the ventriculomegaly induced by hypoxia could affect cognitive function. A novel object recognition test was performed in animals subjected to chronic hypoxia and normoxic controls, as outlined in Figure 3D. In the case of wt young mice, both hypoxic animals and normoxic controls showed a clear preference for the novel object, indicating that the slight increase in the ventricular volume associated with chronic hypoxia did not alter the ability to remember the sample object and identify the new one. In contrast, when the same experimental procedure was applied to aged wt mice, normoxic controls still showed a clear preference for the novel object, but hypoxic animals failed to exhibit any predilection for the new object. This suggests that cognitive deterioration is induced by hypoxia in aged animals, attributable to the increase observed in both total ventricular volume and IVP. Interestingly, and in agreement with the protection against hypoxia-induced hydrocephalus observed in aged AQP4$^{-/-}$ mice, the lack of AQP4 also protects the aged animals from cognitive impairment induced by chronic hypoxia (Fig. 3D, bars graph). Taken together, these data clearly indicate that chronic

hypoxia induces hydrocephalus in aged animals through AQP4, with a moderate increase in IVP, leading to cognitive deterioration.

3.4. CSF outflow rate is affected by aging and hypoxia.

Given the key participation of AQP4 in the ventricular CSF overload under hypoxia, we also studied, in wt and AQP4$^{-/-}$ mice, whether hypoxia and aging were able to modify CSF outflow and ventricular compliance. To that end, pressure-dependent CSF outflow was measured as described elsewhere [14]. As indicated in Figure 4A, artificial CSF was infused into the lateral ventricles and steady state IVP values were recorded as a function of the CSF perfusion rate. Using this experimental procedure, measurements of CSF outflow were performed in wt and AQP4$^{-/-}$ mice (young and aged) exposed to normoxia or hypoxia (Fig. 4B-E and Supp. Mat. 4). Comparison of slopes indicated no significant differences between the pressure-dependent CSF outflow in wt and AQP4$^{-/-}$ young mice in normoxia (Figure 4B); and neither were changes observed in the outflow rates in these animals after the hypoxic treatment (Supp. Mat. 4). Conversely, a clear reduction in slope was found in both wt and AQP4$^{-/-}$ aged animals compared to young ones, that was even more marked after hypoxia treatment (Fig. 4C-E); this indicates that a significant reduction in pressure-dependent CSF outflow is produced over the course of aging, and that this is exacerbated by chronic hypoxia.

In addition to the analysis of the CSF outflow, ventricular compliance (C_v) after the influx of a constant volume (1.75 μl) was evaluated in the experimental groups described before (C_v = 1.75 μl/ ΔP). The induced increase in pressure (ΔP) was clearly larger in aged animals, and it was significantly amplified under chronic hypoxia (Fig. 4F,G), implying therefore a reduction on C_v. Similar to the observations concerning CSF outflow, no significant differences were detected in the ventricular compliance between young wt or AQP4$^{-/-}$ mice exposed to normoxia or hypoxia (Fig. 4G). In brief, these experiments indicate that aging of animals produces a reduction in CSF outflow and ventricular compliance, which is greater under chronic hypoxia. Interestingly, the analysis performed on wt or AQP4$^{-/-}$ mice suggests that the effects of aging and hypoxia on outflow rate and cerebral distensibility are independent of the presence of AQP4 (Fig. 4E,G).

3.5. AQPs expression and their regulation by hypoxia in the brain of aged mice

The expression of brain AQPs was analyzed from two perspectives, examining first the effect of hypoxia in young animals (previously shown in Fig.1) and then the regulation associated with aging and hypoxia (Fig. 5 and Supp. Mat. 5). Consistent with our own results presented above, in aged animals, AQP1 expression was only detected in the choroid plexus, and hypoxia did not affect the expression of this protein in this tissue (Fig. 5A,B). By contrast, the analysis of AQP4 expression in the choroid plexus showed that both mRNA (Fig. 5A) and protein (Fig. 5B) levels were higher in aged mice, with an undetectable signal in young animals and pronounced signal in aged mice, that was even higher after the hypoxic treatment. Further, the levels of AQP4 mRNA (Fig. 5A) and protein (Fig. 5C,D) in brain cortex were higher in aged animals. Curiously, in aged mice the hypoxic treatment (5 days, 10% O_2) induced a slight reduction in the expression of both mRNA (Fig. 5A) and protein (Fig. 5D), although their levels remained 2-fold higher than those observed in young animals. Detailed immunofluorescence analysis was performed of GFAP and AQP4 distribution in the brain cortex (Figure 5C,D). GFAP expression in astrocytes from inner layers was higher in normoxic aged mice than young controls, but the chronic hypoxia treatment slightly increased the GFAP expression in both inner and outer cortical layers. Regarding AQP4, the expression was significantly higher in the aged mice, both in normoxia and hypoxia, across the complete cortical area than in the young animals.

Taken together, the histological and MRI analysis suggest that under chronic hypoxia, the higher levels of AQP4 found in aged brains in the choroid plexus and cortex, both areas associated with CSF generation [35, 47], facilitate the overloading of ventricles with CSF. In addition, measurements of CSF outflow and ventricular compliance indicate that both aging and chronic hypoxia diminish CSF drainage and brain distensibility, contributing to the development of hydrocephalus and significant cognitive deficits.

4. DISCUSSION

Given their function and strategic location in tissues limiting the CSF-brain interface, AQPs have been extensively associated with the production and

absorption of CSF. Numerous studies in various different animal models have indicated that AQP1 and AQP4 contribute to hydrocephalus, a disorder characterized by CSF accumulation in the ventricular system and subarachnoid space [17] [10, 16, 48]. Further, regulation of the expression of cerebral AQPs has been extensively demonstrated by using experimental approaches to produce hypoxia or ischemia including traumatic brain injury and cerebral artery occlusion [49, 50], or just exposure of animals to low oxygen tension [33, 39, 45, 51] and by comparing young and aging animals [35]. In the present work, we performed experiments to explore whether there is a link between hypoxia, AQPs and aged-related hydrocephalus, and the evidence supporting this link are discussed.

We analyzed how AQPs modify their expression in response to chronic hypoxia and whether increases in ventricular volume, as an indicator of greater production of CSF, were occurring in parallel. In line with the “classical” idea that AQP1 in the choroid plexus plays a major role in the production of CSF [52], we expected that hypoxia would preferentially affect expression of AQP1. But on the contrary, although hypoxia was followed by a slight increase in both AQPs in young animals, the only significant increase observed was in AQP4. In normoxia, AQP1 was the AQP most abundantly expressed in the choroid plexus; however, under chronic hypoxia, while AQP1 levels remained almost unchanged, AQP4 passed from being hardly detectable in the choroid plexus to being a moderately expressed protein. In the other brain tissues analyzed, only a transient modification of AQP4 expression was observed in the cortex after 48 hours of hypoxia (Figure 1B-C, Supplementary Fig 1).

The analysis of whether changes in the expression of AQPs in the choroid plexus and other limiting tissues (cells adjacent to brain vasculature, the blood-brain or blood-CSF barriers and ependymal cells bordering the ventricular system) could be involved in a larger hypoxic-dependent production of CSF led to two important findings: first, that hypoxia induces an increase in ventricular volume (likely due to greater production of CSF); and second, that AQP4 channels, and not AQP1 channels, are mainly responsible for the increase in CSF formation. The classic model to explain CSF formation and circulation is currently challenged by a new concept proposing that CSF is produced and absorbed throughout the entire CSF system, and the contribution of the fluid in

the pericapillary space (Virchow-Robin space) to the filtration and reabsorption of CSF is proportionally much larger than that of the choroid plexus alone [52, 53]. The results we present here are fully compatible with this hypothesis of Oreskovic and Klarica and are in agreement with results of Igarashi et al. [54], who found that, following intravenous injection of $H_2{}^{17}O$, water entry into the brain is conducted by AQP4 and not AQP1.

How can hypoxia increase the ventricle CSF load, contributing to a hydrocephalic condition? And in what way do AQPs participate in this process? These were basic questions that emerged from our findings. Previous studies had pointed to hypoxia among the potential causes for hydrocephalus and edema [51, 55, 56]; and increases in brain parenchyma volume and brain swelling in response to acute hypoxia had also been noted [57]. Equivalent to the hyperemic response to ischemia seen in several organs [58, 59], an increment in cerebral blood flow (CBF) occurs in hypoxia as a compensatory mechanism to ensure oxygen supply to the brain. Thus, we postulate that the increase in CSF production observed in hypoxia is a direct consequence of the larger plasma filtration produced by the increase in hydrostatic pressure due to the overload of cerebral blood volume. The observed AQP4 overexpression in the choroid plexus induced by hypoxia will certainly contribute to the greater filtration that occurs during the hyperemic response. Nonetheless, considering that the contact surface between capillaries in the brain parenchyma is vastly larger than that in the choroid plexus [53], one should expect that most of the filtration would occur from capillaries in brain parenchyma. Then, interstitial fluid (ISF) would move to CSF space, driven by the low value of hydrostatic pressure in the CSF compartment, traversing AQP4 present in the pericapillary astrocyte foot processes, astrocytes of the pia mater, interstitial space, and ependymal cells. Consistent with this view, data reported by Ilif et al. [60] indicates that perivascular astroglial AQP4 facilitates the outflow of subarachnoid CSF from para-arterial spaces into the brain interstitial parenchyma, and the resulting ISF clearance, by entrance of the fluid into the para-venous space. Differences in pressure between the arterial and venous extremes would drive the fluid and would favor clearance of solutes in a similar way to a lymphatic system, that is, through the so-called “glymphatic system” [60, 61]. In line with this, the results presented here support the view that AQP4 makes an important contribution to

CSF formation independently and additional to choroid plexus secretion, and allow us to propose AQP4 as a critical therapeutic target, whose inhibition maybe desirable in forms of hydrocephalus involving overproduction of CSF, such as those that result from hypoxic or ischemic conditions.

Another important finding of our study should be highlighted, namely, that there is a resemblance between the hydrocephalic state induced in aged animals by chronic hypoxia and some of the main symptoms of iNPH. Features of adult chronic hydrocephalus depicted in our experimental model include increased ventricle size, a slight increase in intracranial pressure, cognitive deficits and alterations in the cerebral distensibility. This makes us believe that aged mice chronically treated with hypoxia represent an excellent experimental model to study pathophysiological features of iNPH and potential therapeutic options for this disease.

From a mechanistic point of view, the ventriculomegaly observed in aged wt mice, but not in aged AQP4$^{-/-}$ mice, is probably the result of a combination of two factors. Firstly, a greater production of CSF is critically related to the increase in blood flow under chronic hypoxia [57, 62-64] and facilitated by the larger amount of AQP4 found in the cortex and choroid plexus of aged animals. Secondly, but even more importantly, a reduced evacuation of CSF and altered ventricular compliance is associated with aging and is exacerbated by hypoxia (Fig. 6). In that respect, our results, and those of other authors, firmly sustain the view that a dysfunctional CSF outflow system contributes to hydrocephalic conditions. Altered expression and delocalization of cortical perivascular AQP4 have been observed in aged brains of both humans [35] and other animals [47] and are associated with the impairment of effective removal of CSF in both cases. Hence, the more severe astrogliosis we observed in the cortex of aged hypoxic brains may also be associated with a loss of perivascular AQP4 polarization and reduced CSF outflow. The growth in CSF production after exposure to hypoxia was only accompanied by an increase in IVP in aged animals, in which a reduced CSF evacuation and reduced compliance of the ventricular system help to explain the high IVP values. In aged animals, defects in the evacuation of CSF, produced by a process similar to the age-related dysfunctional fibrosis of *Aracnoides* granulations observed in humans [65, 66], by reduced compliance of the ventricular system, and/or by impaired functioning

of the glymphatic system, would contribute to the pronounced ventriculomegaly and high IVP values.

Cognitive deterioration observed in aged hypoxic mice can be expected to be produced by mechanical compression of neuronal circuits critical for memory consolidation due to the edema and ventriculomegaly, although alterations in the glymphatic system and the reduced clearance of CSF could also be related to these cognitive deficits [60, 67]. Signs of reduced glymphatic clearance have been observed in patients with iNPH by gadobutrol-enhanced MRI and allow authors to propose that dementia in these patients may be associated with impaired glymphatic function [68]. Additionally, it has been proposed that altered clearance of CSF and β-amyloid proteins in aged brains contributes to the cognitive deterioration observed in patients with Alzheimer disease [35, 60].

In conclusion, the present study demonstrates, for the first time, that hypoxia and aging (through a greater but disorganized presence of AQP4 channels, lower CSF evacuation rate and reduced cerebral compliance) act synergistically to produce hydrocephalus in mice. Our results suggest a need to develop pharmacological interventions aiming to regulate AQP4 channel transport and such interventions should be tested in future experiments investigating the onset of hydrocephalus or potential treatment strategies. In relation to this, acetazolamide, an inhibitor of AQP4 water flux [69] has been used in various different hydrocephalic conditions [70], including patients with iNPH, showing clear beneficial effects [71, 72]. Finally, from a clinical point of view our experimental results suggest that a hypoxic situation could have a prominent role in the onset of adult hydrocephalus.

ACKNOWLEDGMENTS

This study has been supported by grants FIS: PI12/01882 and PI16/00493 from the Spanish Ministry of Economy and Competitiveness, co-financed by the Carlos III Health Institute (ISCIII) and European Regional Development Fund (FEDER). JLTC was partially supported by the Regional Government of Andalusia and FEDER funds through a program for recruitment of young researchers.

CONFLICT OF INTEREST

The authors declare that they have no conflicts of interest.

ETHICAL APPROVAL

All procedures in studies involving animals were performed in accordance with the ethical standards of the institution at which the studies were conducted.

REFERENCES

[1] A. Wald, G.M. Hochwald, M. Gandhi, Evidence for the movement of fluid, macromolecules and ions from the brain extracellular space to the CSF, Brain Res, 151 (1978) 283-290.
[2] C.E. Johanson, Ventricles and CSF. In: Neuroscience in Medicine, Philadelphia, 1995.
[3] T.H. Milhorat, M.K. Hammock, J.D. Fenstermacher, V.A. Levin, Cerebrospinal fluid production by the choroid plexus and brain, Science, 173 (1971) 330-332.
[4] M.B. Segal, M. Pollay, The secretion of cerebrospinal fluid, Experimental Eye Research, 25 (1977) 127-148.
[5] H. Davson, G. Hollingsworth, M.B. Segal, The Mechanism of Drainage of the Cerebrospinal Fluid, Brain, 93 (1970) 665-678.
[6] K. Welch, Secretion of Cerebrospinal Fluid by Choroid Plexus of the Rabbit, Am J Physiol, 205 (1963) 617-624.
[7] H. Tumani, A. Huss, F. Bachhuber, The cerebrospinal fluid and barriers - anatomic and physiologic considerations, Handb Clin Neurol, 146 (2017) 21-32.
[8] M. Amiry-Moghaddam, O.P. Ottersen, The molecular basis of water transport in the brain, Nat Rev Neurosci, 4 (2003) 991-1001.
[9] M. Zelenina, Regulation of brain aquaporins, Neurochem Int, 57 (2010) 468-488.
[10] M.C. Papadopoulos, A.S. Verkman, Aquaporin water channels in the nervous system, Nat Rev Neurosci, 14 (2013) 265-277.
[11] A.S. Verkman, Physiological importance of aquaporin water channels, Ann Med, 34 (2002) 192-200.
[12] S. Nielsen, B.L. Smith, E.I. Christensen, P. Agre, Distribution of the aquaporin CHIP in secretory and resorptive epithelia and capillary endothelia, Proceedings of the National Academy of Sciences, 90 (1993) 7275-7279.
[13] K. Oshio, D.K. Binder, Y. Liang, A. Bollen, B. Feuerstein, M.S. Berger, G.T. Manley, Expression of the Aquaporin-1 Water Channel in Human Glial Tumors, Neurosurgery, 56 (2005) 375-381.
[14] K. Oshio, H. Watanabe, Y. Song, A.S. Verkman, G.T. Manley, Reduced cerebrospinal fluid production and intracranial pressure in mice lacking choroid plexus water channel Aquaporin-1, FASEB J, 19 (2005) 76-78.
[15] T. Speake, C. Whitwell, H. Kajita, A. Majid, P.D. Brown, Mechanisms of CSF secretion by the choroid plexus, Microsc Res Tech, 52 (2001) 49-59.
[16] E.A. Nagelhus, O.P. Ottersen, Physiological roles of aquaporin-4 in brain, Physiol Rev, 93 (2013) 1543-1562.

[17] D. Wang, M. Nykanen, N. Yang, D. Winlaw, K. North, A.S. Verkman, B.K. Owler, Altered cellular localization of aquaporin-1 in experimental hydrocephalus in mice and reduced ventriculomegaly in aquaporin-1 deficiency, Mol Cell Neurosci, 46 (2011) 318-324.
[18] J. Badaut, F. Lasbennes, P.J. Magistretti, L. Regli, Aquaporins in brain: distribution, physiology, and pathophysiology, J Cereb Blood Flow Metab, 22 (2002) 367-378.
[19] T. Tourdias, I. Dragonu, Y. Fushimi, M.S. Deloire, C. Boiziau, B. Brochet, C. Moonen, K.G. Petry, V. Dousset, Aquaporin 4 correlates with apparent diffusion coefficient and hydrocephalus severity in the rat brain: a combined MRI-histological study, Neuroimage, 47 (2009) 659-666.
[20] M.J. Schmidt, C. Rummel, J. Hauer, M. Kolecka, N. Ondreka, V. McClure, J. Roth, Increased CSF aquaporin-4, and interleukin-6 levels in dogs with idiopathic communicating internal hydrocephalus and a decrease after ventriculo-peritoneal shunting, Fluids Barriers CNS, 13 (2016) 12.
[21] K. Aghayev, E. Bal, T. Rahimli, M. Mut, S. Balci, F. Vrionis, N. Akalan, Aquaporin-4 expression is not elevated in mild hydrocephalus, Acta Neurochir (Wien), 154 (2012) 753-759; discussion 759.
[22] A.D. Skjolding, A.V. Holst, H. Broholm, H. Laursen, M. Juhler, Differences in distribution and regulation of astrocytic aquaporin-4 in human and rat hydrocephalic brain, Neuropathol Appl Neurobiol, 39 (2013) 179-191.
[23] L.K. Page, Cerebrospinal fluid and extracellular fluid: their relationship to pressure and duration of canine hydrocephalus, Childs Nerv Syst, 1 (1985) 12-17.
[24] O. Bloch, K.I. Auguste, G.T. Manley, A.S. Verkman, Accelerated progression of kaolin-induced hydrocephalus in aquaporin-4-deficient mice, J Cereb Blood Flow Metab, 26 (2006) 1527-1537.
[25] M.C. Papadopoulos, G.T. Manley, S. Krishna, A.S. Verkman, Aquaporin-4 facilitates reabsorption of excess fluid in vasogenic brain edema, FASEB J, 18 (2004) 1291-1293.
[26] M.Y. Kalani, A.S. Filippidis, H.L. Rekate, Hydrocephalus and aquaporins: the role of aquaporin-1, Acta Neurochir Suppl, 113 (2012) 51-54.
[27] A.S. Filippidis, M.Y. Kalani, H.L. Rekate, Hydrocephalus and aquaporins: the role of aquaporin-4, Acta Neurochir Suppl, 113 (2012) 55-58.
[28] A.J. Espay, G.A. Da Prat, A.K. Dwivedi, F. Rodriguez-Porcel, J.E. Vaughan, M. Rosso, J.L. Devoto, A.P. Duker, M. Masellis, C.D. Smith, G.T. Mandybur, A. Merola, A.E. Lang, Deconstructing normal pressure hydrocephalus: Ventriculomegaly as early sign of neurodegeneration, Ann Neurol, 82 (2017) 503-513.
[29] H. Wessling, C.L. Simosono, M. Escosa-Bage, P. de las Heras-Echeverria, Continuous cerebral PtO2 measurements in awake patients as a diagnostic tool in suspected chronic adult hydrocephalus--a retrospective study of 10 cases, Acta Neurochir (Wien), 149 (2007) 239-244; discussion 244.
[30] S.M. Dombrowski, A. Deshpande, C. Dingwall, A. Leichliter, Z. Leibson, M.G. Luciano, Chronic hydrocephalus-induced hypoxia: increased expression of VEGFR-2+ and blood vessel density in hippocampus, Neuroscience, 152 (2008) 346-359.
[31] J.Y. Ding, C.W. Kreipke, S.L. Speirs, P. Schafer, S. Schafer, J.A. Rafols, Hypoxia-inducible factor-1alpha signaling in aquaporin upregulation after traumatic brain injury, Neurosci Lett, 453 (2009) 68-72.

[32] N. Yamamoto, K. Yoneda, K. Asai, K. Sobue, T. Tada, Y. Fujita, H. Katsuya, M. Fujita, N. Aihara, M. Mase, K. Yamada, Y. Miura, T. Kato, Alterations in the expression of the AQP family in cultured rat astrocytes during hypoxia and reoxygenation, Brain Res Mol Brain Res, 90 (2001) 26-38.
[33] I. Abreu-Rodriguez, R.o. Sanchez Silva, A.P. Martins, G.a. Soveral, J.J. Toledo-Aral, J. Lopez-Barneo, M. Echevarria, Functional and Transcriptional Induction of Aquaporin-1 Gene by Hypoxia; Analysis of Promoter and Role of Hif-1à, PLoS ONE, 6 (2011) e28385.
[34] M. Echevarria, A.M. Muñoz-Cabello, R.o. Sanchez-Silva, J.J. Toledo-Aral, J. Lopez-Barneo, Development of Cytosolic Hypoxia and Hypoxia-inducible Factor Stabilization Are Facilitated by Aquaporin-1 Expression, Journal of Biological Chemistry, 282 (2007) 30207-30215.
[35] D.M. Zeppenfeld, M. Simon, J.D. Haswell, D. D'Abreo, C. Murchison, J.F. Quinn, M.R. Grafe, R.L. Woltjer, J. Kaye, J.J. Iliff, Association of Perivascular Localization of Aquaporin-4 With Cognition and Alzheimer Disease in Aging Brains, JAMA Neurol, 74 (2017) 91-99.
[36] P. Hellstrom, P. Klinge, J. Tans, C. Wikkelso, A new scale for assessment of severity and outcome in iNPH, Acta Neurol Scand, 126 (2012) 229-237.
[37] M. Hashimoto, M. Ishikawa, E. Mori, N. Kuwana, I.o.n.i. Study of, Diagnosis of idiopathic normal pressure hydrocephalus is supported by MRI-based scheme: a prospective cohort study, Cerebrospinal Fluid Res, 7 (2010) 18.
[38] T. Ma, B. Yang, A. Gillespie, E.J. Carlson, C.J. Epstein, A.S. Verkman, Generation and phenotype of a transgenic knockout mouse lacking the mercurial-insensitive water channel aquaporin-4, J Clin Invest, 100 (1997) 957-962.
[39] A. Galan-Cobo, R. Ramirez-Lorca, J.J. Toledo-Aral, M. Echevarria, Aquaporin-1 plays important role in proliferation by affecting cell cycle progression, Journal of Cellular Physiology, 231 (2016) 243-256.
[40] A.M. Muñoz-Cabello, J. Villadiego, J.J. Toledo-Aral, J. Lopez-Barneo, M. Echevarr¡a, AQP1 mediates water transport in the carotid body, Pflügers Archiv - European Journal of Physiology, 459 (2010) 775-783.
[41] A.B. Munoz-Manchado, J. Villadiego, N. Suarez-Luna, A. Bermejo-Navas, P. Garrido-Gil, J.L. Labandeira-Garcia, M. Echevarria, J. Lopez-Barneo, J.J. Toledo-Aral, Neuroprotective and reparative effects of carotid body grafts in a chronic MPTP model of Parkinson's disease, Neurobiol Aging, 34 (2013) 902-915.
[42] A.B. Munoz-Manchado, J. Villadiego, S. Romo-Madero, N. Suarez-Luna, A. Bermejo-Navas, J.A. Rodriguez-Gomez, P. Garrido-Gil, J.L. Labandeira-Garcia, M. Echevarria, J. Lopez-Barneo, J.J. Toledo-Aral, Chronic and progressive Parkinson's disease MPTP model in adult and aged mice, J Neurochem, 136 (2016) 373-387.
[43] J. Villadiego, A. Labrador-Garrido, J.M. Franco, M. Leal-Lasarte, E.J. De Genst, C.M. Dobson, D. Pozo, J.J. Toledo-Aral, C. Roodveldt, Immunization with alpha-synuclein/Grp94 reshapes peripheral immunity and suppresses microgliosis in a chronic Parkinsonism model, Glia, 66 (2018) 191-205.
[44] A. Wolf, B. Bauer, E.L. Abner, T. Ashkenazy-Frolinger, A.M. Hartz, A Comprehensive Behavioral Test Battery to Assess Learning and Memory in 129S6/Tg2576 Mice, PLoS One, 11 (2016) e0147733.
[45] S.J. Chen, J.F. Yang, F.P. Kong, J.L. Ren, K. Hao, M. Li, Y. Yuan, X.C. Chen, R.S. Yu, J.F. Li, G. Leng, X.Q. Chen, J.Z. Du, Overactivation of

corticotropin-releasing factor receptor type 1 and aquaporin-4 by hypoxia induces cerebral edema, Proc Natl Acad Sci U S A, 111 (2014) 13199-13204.
[46] A. Zeisel, A.B. Munoz-Manchado, S. Codeluppi, P. Lonnerberg, G. La Manno, A. Jureus, S. Marques, H. Munguba, L. He, C. Betsholtz, C. Rolny, G. Castelo-Branco, J. Hjerling-Leffler, S. Linnarsson, Brain structure. Cell types in the mouse cortex and hippocampus revealed by single-cell RNA-seq, Science, 347 (2015) 1138-1142.
[47] B.T. Kress, J.J. Iliff, M. Xia, M. Wang, H.S. Wei, D. Zeppenfeld, L. Xie, H. Kang, Q. Xu, J.A. Liew, B.A. Plog, F. Ding, R. Deane, M. Nedergaard, Impairment of paravascular clearance pathways in the aging brain, Ann Neurol, 76 (2014) 845-861.
[48] B. Desai, Y. Hsu, B. Schneller, J.G. Hobbs, A.I. Mehta, A. Linninger, Hydrocephalus: the role of cerebral aquaporin-4 channels and computational modeling considerations of cerebrospinal fluid, Neurosurg Focus, 41 (2016) E8.
[49] C. Zhang, J. Chen, H. Lu, Expression of aquaporin-4 and pathological characteristics of brain injury in a rat model of traumatic brain injury, Mol Med Rep, 12 (2015) 7351-7357.
[50] D.S. Frydenlund, A. Bhardwaj, T. Otsuka, M.N. Mylonakou, T. Yasumura, K.G. Davidson, E. Zeynalov, O. Skare, P. Laake, F.M. Haug, J.E. Rash, P. Agre, O.P. Ottersen, M. Amiry-Moghaddam, Temporary loss of perivascular aquaporin-4 in neocortex after transient middle cerebral artery occlusion in mice, Proc Natl Acad Sci U S A, 103 (2006) 13532-13536.
[51] D.C. Curran-Everett, J. Iwamoto, M.P. Meredith, J.A. Krasney, Intracranial pressures and O2 extraction in conscious sheep during 72 h of hypoxia, Am J Physiol, 261 (1991) H103-109.
[52] D. Oreskovic, M. Rados, M. Klarica, Role of choroid plexus in cerebrospinal fluid hydrodynamics, Neuroscience, 354 (2017) 69-87.
[53] D. Oreskovic, M. Klarica, Development of hydrocephalus and classical hypothesis of cerebrospinal fluid hydrodynamics: facts and illusions, Prog Neurobiol, 94 (2011) 238-258.
[54] H. Igarashi, M. Tsujita, I.L. Kwee, T. Nakada, Water influx into cerebrospinal fluid is primarily controlled by aquaporin-4, not by aquaporin-1: 17O JJVCPE MRI study in knockout mice, Neuroreport, 25 (2014) 39-43.
[55] D.E. Sakas, H.L. Whitwell, R.J. Watkins, D.J. Beale, Ultra early transient brain swelling following brief intraoperative ischaemia-reperfusion, J Clin Neurosci, 6 (1999) 324-325.
[56] H. Williams, A unifying hypothesis for hydrocephalus and the Chiari malformations part two: The hydrocephalus filling mechanism, Med Hypotheses, 94 (2016) 30-39.
[57] D.J. Dubowitz, E.A. Dyer, R.J. Theilmann, R.B. Buxton, S.R. Hopkins, Early brain swelling in acute hypoxia, J Appl Physiol (1985), 107 (2009) 244-252.
[58] J. Loscalzo, J.A. Vita, Ischemia, hyperemia, exercise, and nitric oxide. Complex physiology and complex molecular adaptations, Circulation, 90 (1994) 2556-2559.
[59] A. Menyhart, D. Zolei-Szenasi, T. Puskas, P. Makra, F. Bari, E. Farkas, Age or ischemia uncouples the blood flow response, tissue acidosis, and direct current potential signature of spreading depolarization in the rat brain, Am J Physiol Heart Circ Physiol, 313 (2017) H328-H337.
[60] J.J. Iliff, M. Wang, Y. Liao, B.A. Plogg, W. Peng, G.A. Gundersen, H. Benveniste, G.E. Vates, R. Deane, S.A. Goldman, E.A. Nagelhus, M.

Nedergaard, A paravascular pathway facilitates CSF flow through the brain parenchyma and the clearance of interstitial solutes, including amyloid beta, Sci Transl Med, 4 (2012) 147ra111.
[61] J.J. Iliff, H. Lee, M. Yu, T. Feng, J. Logan, M. Nedergaard, H. Benveniste, Brain-wide pathway for waste clearance captured by contrast-enhanced MRI, J Clin Invest, 123 (2013) 1299-1309.
[62] E.A. Dyer, S.R. Hopkins, J.E. Perthen, R.B. Buxton, D.J. Dubowitz, Regional cerebral blood flow during acute hypoxia in individuals susceptible to acute mountain sickness, Respir Physiol Neurobiol, 160 (2008) 267-276.
[63] M.H. Wilson, C.H. Imray, A.R. Hargens, The headache of high altitude and microgravity--similarities with clinical syndromes of cerebral venous hypertension, High Alt Med Biol, 12 (2011) 379-386.
[64] J.S. Lawley, B.D. Levine, M.A. Williams, J. Malm, A. Eklund, D.M. Polaner, A.W. Subudhi, P.H. Hackett, R.C. Roach, Cerebral spinal fluid dynamics: effect of hypoxia and implications for high-altitude illness, J Appl Physiol (1985), 120 (2016) 251-262.
[65] K. Akai, S. Uchigasaki, U. Tanaka, A. Komatsu, Normal pressure hydrocephalus. Neuropathological study, Acta Pathol Jpn, 37 (1987) 97-110.
[66] S. Destian, L.A. Heier, R.D. Zimmerman, S. Morgello, M.D. Deck, Differentiation between meningeal fibrosis and chronic subdural hematoma after ventricular shunting: value of enhanced CT and MR scans, AJNR Am J Neuroradiol, 10 (1989) 1021-1026.
[67] W. Peng, T.M. Achariyar, B. Li, Y. Liao, H. Mestre, E. Hitomi, S. Regan, T. Kasper, S. Peng, F. Ding, H. Benveniste, M. Nedergaard, R. Deane, Suppression of glymphatic fluid transport in a mouse model of Alzheimer's disease, Neurobiol Dis, 93 (2016) 215-225.
[68] G. Ringstad, S.A.S. Vatnehol, P.K. Eide, Glymphatic MRI in idiopathic normal pressure hydrocephalus, Brain, 140 (2017) 2691-2705.
[69] Y. Tanimura, Y. Hiroaki, Y. Fujiyoshi, Acetazolamide reversibly inhibits water conduction by aquaporin-4, J Struct Biol, 166 (2009) 16-21.
[70] F. Gao, M. Zheng, Y. Hua, R.F. Keep, G. Xi, Acetazolamide Attenuates Thrombin-Induced Hydrocephalus, Acta Neurochir Suppl, 121 (2016) 373-377.
[71] M. Ivkovic, M. Reiss-Zimmermann, H. Katzen, M. Preuss, I. Kovanlikaya, L. Heier, N. Alperin, K.T. Hoffmann, N. Relkin, MRI assessment of the effects of acetazolamide and external lumbar drainage in idiopathic normal pressure hydrocephalus, Fluids Barriers CNS, 12 (2015) 9.
[72] G.J. Gilbert, N. Alperin, C. Olio, N. Relkin, Low-dose acetazolamide reverses periventricular white matter hyperintensities in iNPH, Neurology, 83 (2014) 1773.

FIGURE LEGENDS

Figure 1. Brain AQP1 and AQP4 expression in mice exposed to hypoxia.

(A) Expression of AQP mRNA in mice exposed to hypoxia (10% O_2, 48 hours) and normoxic controls was analyzed in the choroid plexus (Plx), cortex (Ctx), tissue lining the lateral ($Ep_{Lat.V}$) and 3rd ventricle ($Ep_{3th.V}$), and striatum (Str). 18S

ribosomal RNA was used as housekeeping gene for normalization. (B) AQP1 and AQP4 immunofluorescence images of choroid plexus obtained from mice exposed to normoxia or hypoxia (10% O_2; 48 hours and 5 days). AQP4 expression is notably higher after the hypoxic treatment. (C) Immunofluorescence images of GFAP and AQP4 in brain cortex from the aforementioned experimental groups. (D) Quantification, by optical density, of the GFAP and AQP4 expression in cortex layers I-II and III-VI in the aforementioned groups.

GFAP: glial fibrillary acidic protein. DAPI: 4',6-diamidino-2-phenylindole.

In A and D data are presented as mean ± S.E.M. An unpaired t-test was performed for A and analysis of variance with Bonferroni post hoc test for D. *p<0.05, ** p<0.01 with respect to normoxic controls. $^{\dagger}p<0.05$, $^{\dagger\dagger}p<0.01$, $^{\dagger\dagger\dagger}p<0.001$ differences between cortical layers I-II and III-IV (paired t-test).

Figure 2. Magnetic resonance images and intraventricular pressure of young mice exposed to chronic hypoxia. (A) MRI of brain coronal sections of young wt mice exposed to normoxia or chronic hypoxia (10% O_2, 5 days). (B) Quantification of the ventricular volume from MRI of wt, AQP1$^{-/-}$ and AQP4$^{-/-}$ mice under the experimental conditions indicated in A. (C) Diagram illustrating the procedure to measure the IVP. (D) Values of IVP in wt, AQP1$^{-/-}$ and AQP4$^{-/-}$ mice exposed to hypoxia (10% O2, 5 days) or kept in normoxia.

In B and D data are presented as mean ± S.E.M. An unpaired t-test was performed for B and analysis of variance with Bonferroni post hoc test for D. *p<0.05, with respect to normoxic control mice.

Figure 3. Ventriculomegaly induced by chronic hypoxia in aged animals. (A) MRI of brain coronal sections of aged wt mice exposed to normoxia or chronic hypoxia (10% O_2, 5 days). (B) Quantification of the ventricular volume of young wt and aged wt, AQP1$^{-/-}$ and AQP4$^{-/-}$ mice under the experimental conditions indicated in A. (C) Values of IVP in aged wt, AQP1$^{-/-}$ and AQP4$^{-/-}$ mice, under the aforementioned conditions. (D) Diagram showing the experimental protocol performed to evaluate cognitive function, by novel object recognition, and analysis of the novel object recognition test. Note that in aged mice the hypoxic treatment produces hydrocephalus, manifested by a large

increase in the total ventricular volume (which is dependent on the AQP4 expression) with an increase in the IVP and deterioration in cognitive function.

In B, C and D data are presented as mean ± S.E.M. An unpaired t-test was performed. B and C, *p<0.05, **p<0.01 with respect to normoxic control mice. †p<0.05, ††p<0.01 with respect to wt mice. D, *p<0.05 and ***p<0.001 with respect to the sample object (on the sample trial).

Figure 4. Measurements of CSF outflow rates and ventricular compliance. (A) Schematic representation of the methodology used to measure outflow rate of CSF. (B-E) Outflow rate measurements were performed in young wt and AQP4$^{-/-}$ in normoxia (B); young and aged mice exposed to normoxia or hypoxia (10% O_2, 5 days; C and D for wt and AQP4$^{-/-}$ respectively); and comparison between aged wt and AQP4$^{-/-}$ mice exposed to normoxia or hypoxia (E). Comparison of slopes indicated non-significant differences between the pressure-dependent CSF outflow of experimental groups analyzed in B, but clear reduction in slope in aged mice, compared to young controls, that is even more pronounced in aged hypoxic mice. (F) Diagram outlining the methodology used to analyze the ventricular compliance. (G) Quantitative analysis of the ventricular compliance in wt and AQP4$^{-/-}$ young and aged mice exposed to normoxia or chronic hypoxia.

In B-E data are presented, for each experimental point, as mean ± S.E.M and the linear regression line was extrapolated for each experimental condition. Analysis of variance with Tukey HSD post hoc test **p<0.01 and ***p<0.001 with respect to young wt mice. In G data are presented as mean ± S.E.M. *p<0.05, **p<0.01 and ***p<0.001 with respect to young wt normoxic controls. †p<0.05, ††p<0.01 and †††p<0.001 with respect to young AQP4$^{-/-}$ normoxic mice.

Figure 5. Effect of aging and hypoxia on brain AQP expression. (A) Expression of AQP mRNA was analyzed in wt young, normoxic aged (≥14 months) and hypoxic aged (exposed to 10% O_2, 5 days). Choroid plexus (Plx), cortex (Ctx), ependymal tissue from lateral ventricle ($Ep_{Lat.V}$) and 3rd ventricle ($Ep_{3th.V}$) and striatum (Str) were analyzed separately for mRNA levels of AQP1 and AQP4 by quantitative real-time PCR analysis. 18S ribosomal RNA was

used as housekeeping gene for normalization. (B) Immunofluorescence images for AQP1 and AQP4 of choroid plexus obtained from mice of the aforementioned experimental groups. The level of AQP4 is notably higher in the aged mice, both in normoxia and hypoxia, than in the young controls. (C) Immunofluorescence images of GFAP and AQP4 in brain cortex of mice from the experimental groups indicated in A. (D) Quantification, by optical density, of the GFAP and AQP4 expression in cortex layers I-II and III-VI in the aforementioned groups.

GFAP: glial fibrillary acidic protein. DAPI: 4',6-diamidino-2-phenylindole.

In A and D data are presented as mean ± S.E.M. Analysis of variance with Tukey HSD post hoc test was performed. *$p<0.05$, ***$p<0.001$ with respect to young normoxic controls;$^{\dagger}p<0.05$, $^{\dagger\dagger}p<0.01$, $^{\dagger\dagger\dagger}p<0.001$ differences between cortical layers I-II and III-VI (paired t-test).

Figure 6. Model of age-related hydrocephalus associated with chronic hypoxia.

(A) In young normoxic mice, AQP4 (red channels, present on glial bordering membranes and astrocyte foot processes) and AQP1 (blue channels, expressed on choroid plexus) participate in CSF formation. (B) Chronic hypoxia induces, in young mice, AQP4 expression in the choroid plexus and mild ventriculomegaly dependent on AQP4 expression. (C) In aged normoxic mice, AQP4 expression increased in cortical glial cells and choroid plexus, and CSF outflow and ventricular compliance decreased. (D) Chronic hypoxia in aged mice induces pronounced ventriculomegaly, with increased intraventricular pressure, resulting in cognitive deterioration. This hydrocephalic condition is produced by CSF overload on the ventricles, which is facilitated by the higher amounts of AQP4, the reduced capability to evacuate CSF and the altered ventricular compliance of the aged cerebral parenchyma.

$GFAP^{high}$ astrocytes are represented in green and $GFAP^{low}$ astrocytes in grey.

SUPPLEMENTARY MATERIAL

Supplementary Material-1: Primer sequences used for quantitative PCR.

Supplementary Material-2: Brain AQP1 and AQP4 protein expression in young mice exposed to hypoxia. (A) AQP1 and AQP4 protein expression, measured by Western blot, in the choroid plexus (Plx), cortex (Ctx), ependymal tissue from lateral ventricle ($Ep_{Lat.V}$) and striatum (Str) from normoxic controls and mice exposed to hypoxia (10% O_2; 48 hours). β-actin protein level was used for normalization. (B-D). Immunofluorescence images for AQP4 and GFAP from ependymal tissue from lateral ventricle (B), ependymal tissue from 3rd ventricle (C) and striatum (D) obtained from mice exposed to hypoxia (10% O_2; 48 hours and 5 days) and normoxic controls.

Supplementary Material-3: Systemic arterial pressure measurements in young and aged wt, AQP1$^{-/-}$ and AQP4$^{-/-}$ mice exposed to hypoxia or normoxia. Values (as mean ± S.E.M) of systolic, diastolic and mean blood pressure of young (A) and aged (B) wt, AQP1$^{-/-}$ and AQP4$^{-/-}$ mice exposed to normoxia or chronic hypoxia (10% O_2; 5 days).

Supplementary Material-4: CSF outflow rates from wt and AQP4$^{-/-}$ mice exposed to hypoxia and normoxic controls. Outflow rate measurements in young wt (A) and AQP4$^{-/-}$ (B) in normoxia or chronic hypoxia (10% O_2; 5 days). Comparison of slopes indicated non-significant differences between the pressure-dependent CSF outflow in the experimental groups analyzed.
Data are presented, for each experimental point, as mean ± S.E.M and the linear regression line was extrapolated for each experimental condition.

Supplementary Material-5: Effect of aging and hypoxia on brain AQP4 expression. (A-C) Immunofluorescence images for AQP4 and GFAP of ependymal tissue from lateral ventricle ($Ep_{Lat.V}$; A), 3rd ventricle ($Ep_{3th.V}$; B) and striatum (Str; C) obtained from young normoxic, aged normoxic and aged hypoxic (10% O_2; 5 days) mice.

Figure 1

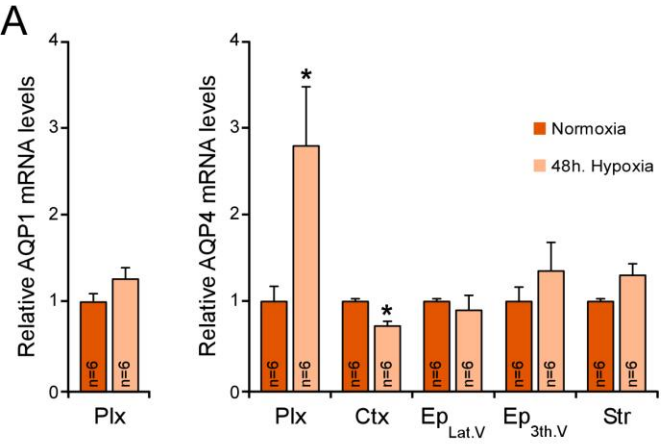
A
Relative AQP1 mRNA levels
Relative AQP4 mRNA levels
Normoxia
48h. Hypoxia
Plx
Ctx
Ep Lat.V
Ep 3th.V
Str
n=6

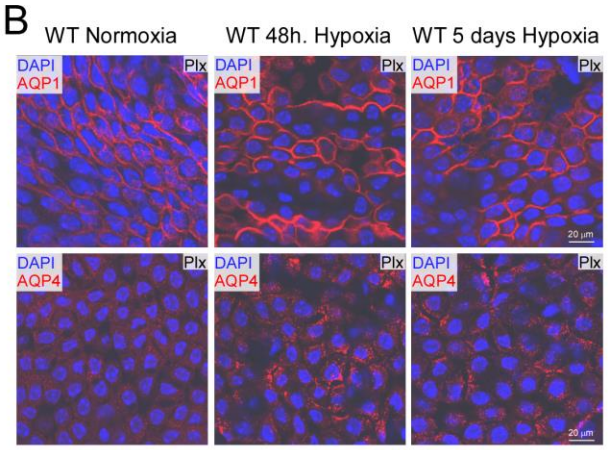
B
WT Normoxia
WT 48h. Hypoxia
WT 5 days Hypoxia
DAPI
AQP1
AQP4
Plx
20 µm

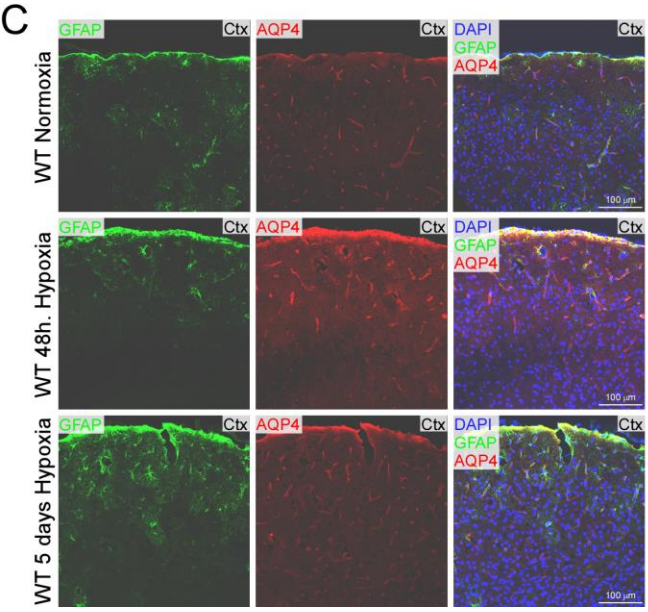
C
WT Normoxia
WT 48h. Hypoxia
WT 5 days Hypoxia
GFAP
AQP4
DAPI
Ctx
100 µm

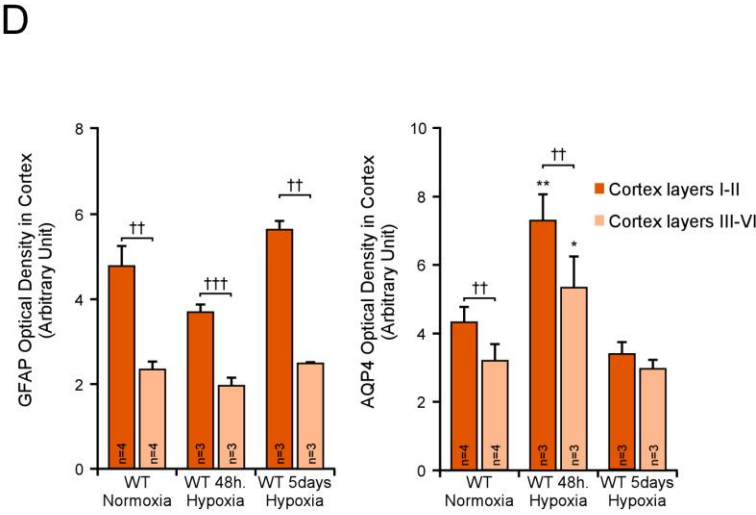
D
GFAP Optical Density in Cortex (Arbitrary Unit)
AQP4 Optical Density in Cortex (Arbitrary Unit)
Cortex layers I-II
Cortex layers III-VI
WT Normoxia
WT 48h. Hypoxia
WT 5days Hypoxia
n=4
n=3

Figure 2

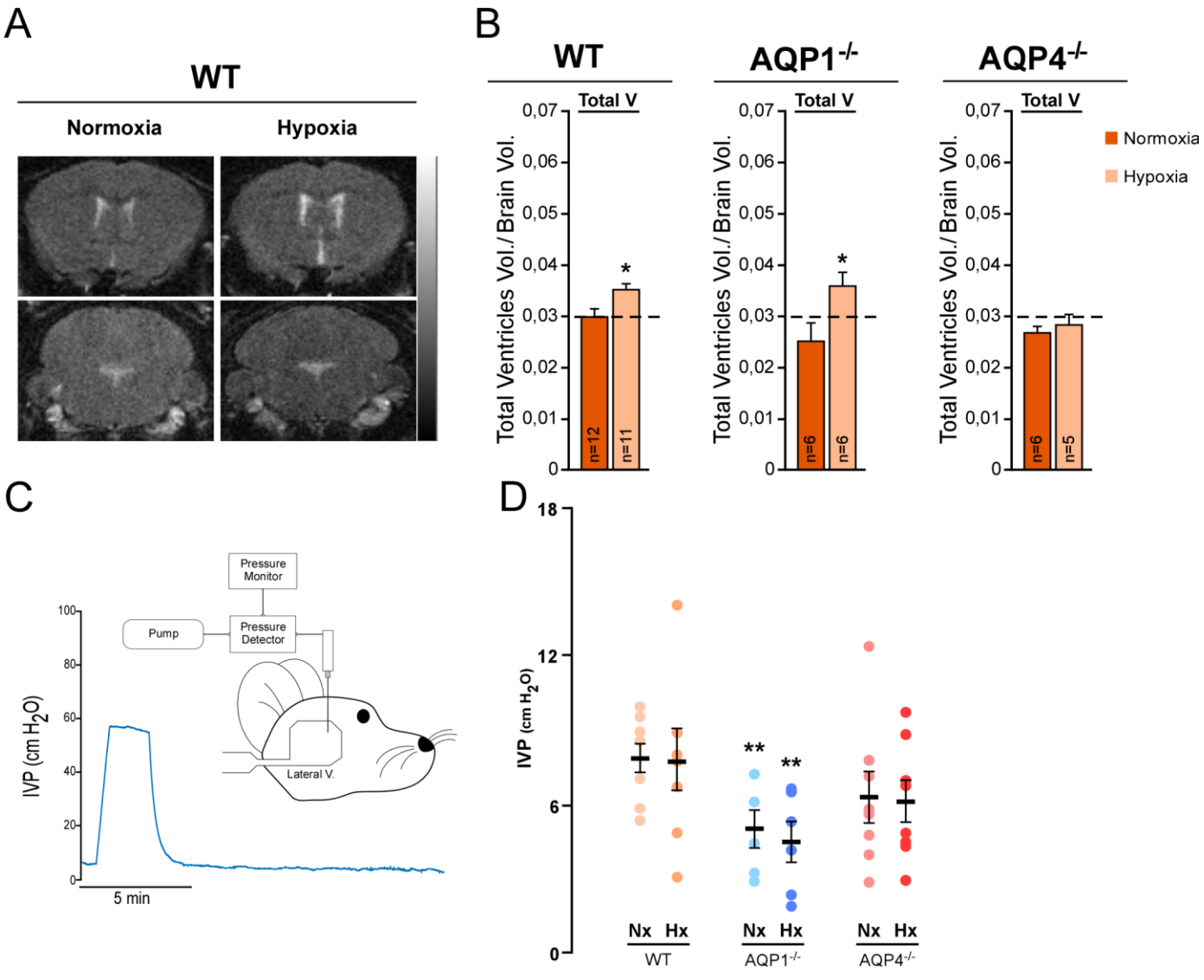
A
WT
Normoxia
Hypoxia
B
WT
AQP1-/-
AQP4-/-
Total V
Total Ventricles Vol./Brain Vol.
0,07
0,06
0,05
0,04
0,03
0,02
0,01
0
n=12
n=11
n=6
n=6
n=6
n=5
*
Normoxia
Hypoxia
C
Pressure Monitor
Pump
Pressure Detector
Lateral V.
IVP (cm H2O)
100
80
60
40
20
0
5 min
D
IVP (cm H2O)
18
12
6
0
**
**
Nx Hx
WT
Nx Hx
AQP1-/-
Nx Hx
AQP4-/-

Figure 3

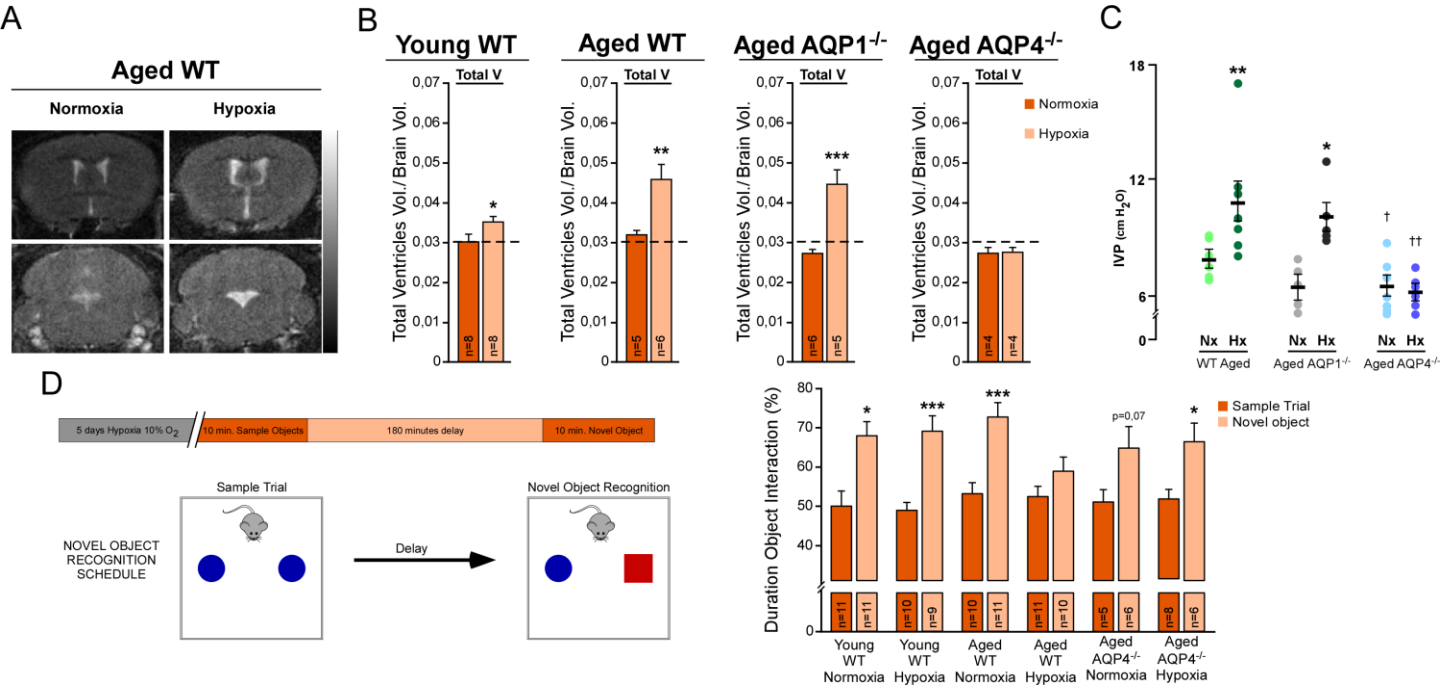
A
Aged WT
Normoxia
Hypoxia
B
Young WT
Aged WT
Aged AQP1-/-
Aged AQP4-/-
Total V
Total Ventricles Vol./Brain Vol.
Normoxia
Hypoxia
C
IVP (cm H2O)
Nx Hx
WT Aged
Aged AQP1-/-
Aged AQP4-/-
D
5 days Hypoxia 10% O2
10 min. Sample Objects
180 minutes delay
10 min. Novel Object
Sample Trial
Novel Object Recognition
NOVEL OBJECT RECOGNITION SCHEDULE
Delay
Duration Object Interaction (%)
Sample Trial
Novel object
p=0.07
Young WT Normoxia
Young WT Hypoxia
Aged WT Normoxia
Aged WT Hypoxia
Aged AQP4-/- Normoxia
Aged AQP4-/- Hypoxia

Figure 4

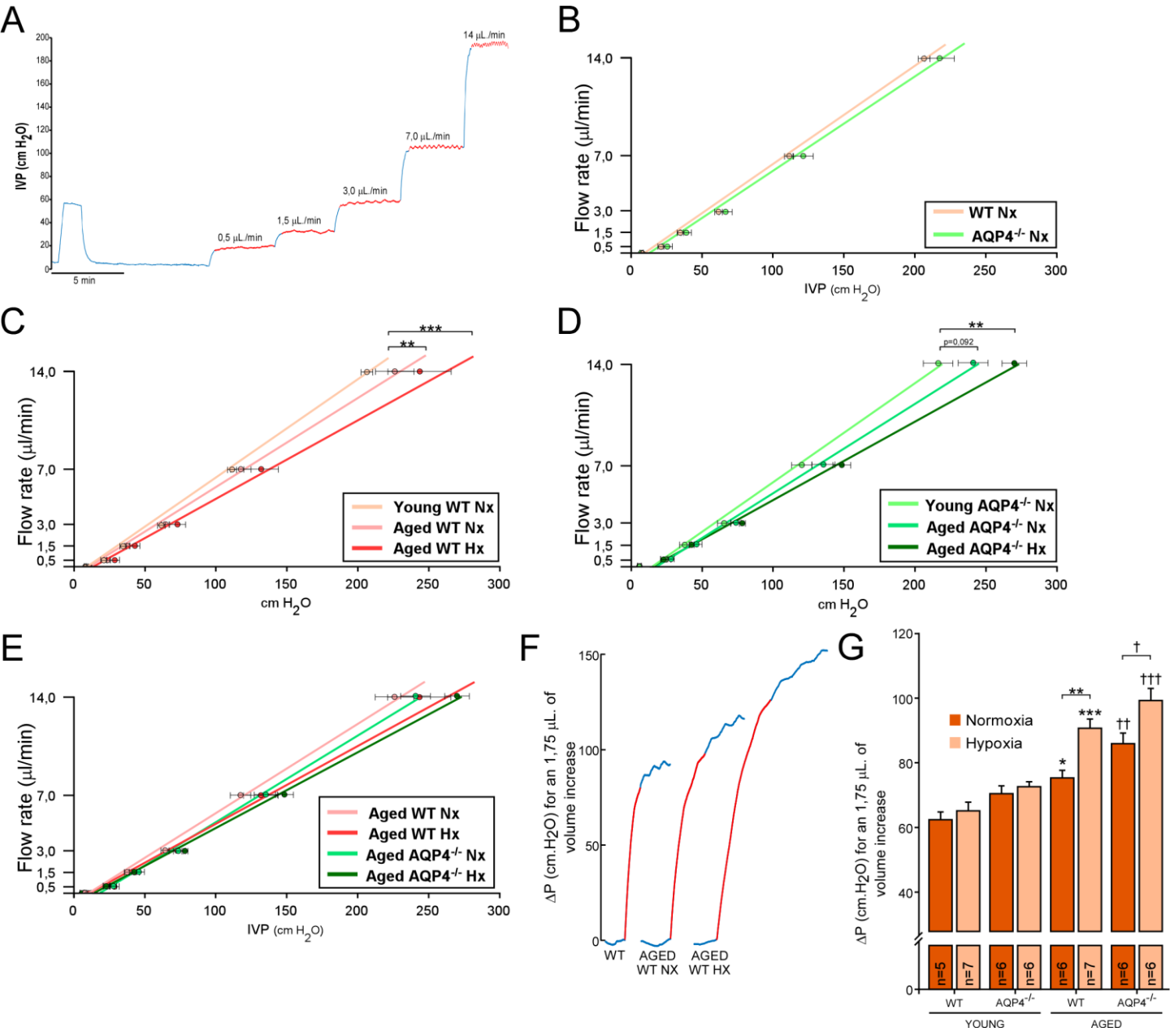
A
IVP (cm H2O)
14 µL./min
7,0 µL./min
3,0 µL./min
1,5 µL./min
0,5 µL./min
5 min
B
Flow rate (µl/min)
IVP (cm H2O)
WT Nx
AQP4-/- Nx
C
Flow rate (µl/min)
cm H2O
Young WT Nx
Aged WT Nx
Aged WT Hx
***
**
D
Flow rate (µl/min)
cm H2O
Young AQP4-/- Nx
Aged AQP4-/- Nx
Aged AQP4-/- Hx
**
p=0,092
E
Flow rate (µl/min)
IVP (cm H2O)
Aged WT Nx
Aged WT Hx
Aged AQP4-/- Nx
Aged AQP4-/- Hx
F
ΔP (cm.H2O) for an 1,75 µL. of volume increase
WT
AGED WT NX
AGED WT HX
G
ΔP (cm.H2O) for an 1,75 µL. of volume increase
Normoxia
Hypoxia
*
**
***
†
††
†††
n=5
n=7
n=6
n=6
n=6
n=7
n=6
n=6
WT
AQP4-/-
WT
AQP4-/-
YOUNG
AGED

Figure 5

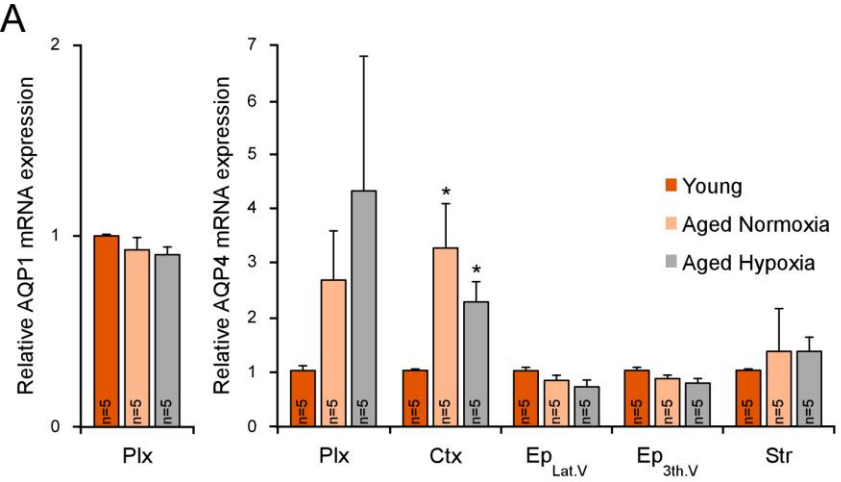
A
Relative AQP1 mRNA expression
Relative AQP4 mRNA expression
Young
Aged Normoxia
Aged Hypoxia
n=5
Plx
Ctx
Ep Lat.V
Ep 3th.V
Str

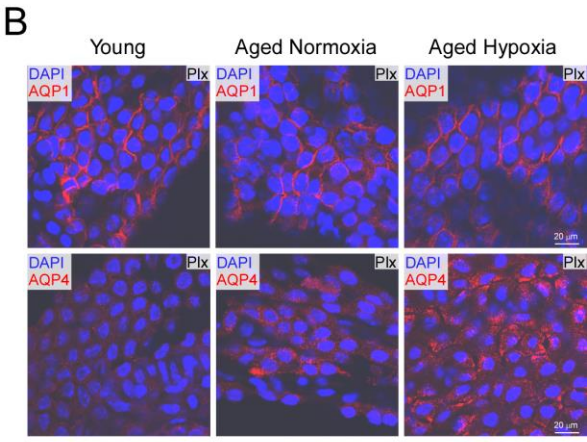
B
Young
Aged Normoxia
Aged Hypoxia
DAPI
AQP1
AQP4
Plx
20 µm

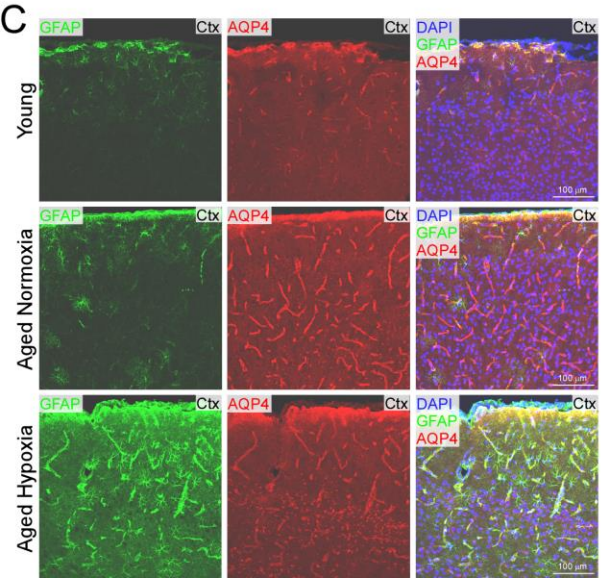
C
GFAP
AQP4
DAPI
Ctx
Young
Aged Normoxia
Aged Hypoxia
100 µm

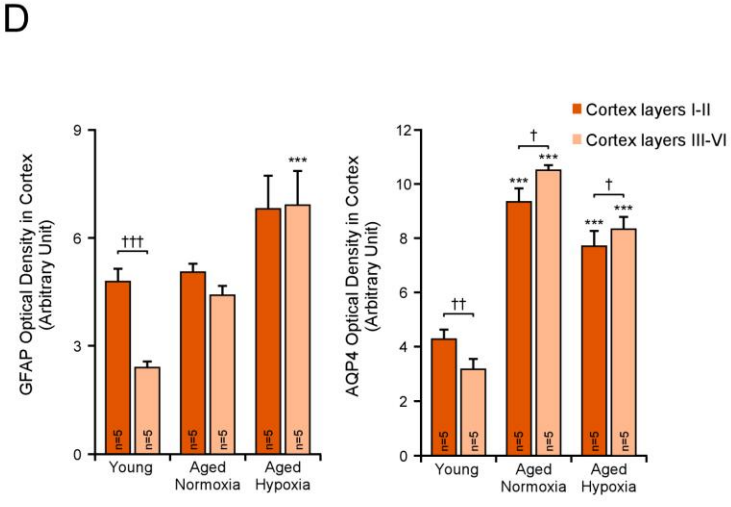
D
GFAP Optical Density in Cortex (Arbitrary Unit)
AQP4 Optical Density in Cortex (Arbitrary Unit)
Cortex layers I-II
Cortex layers III-VI
Young
Aged Normoxia
Aged Hypoxia
n=5

Figure 6

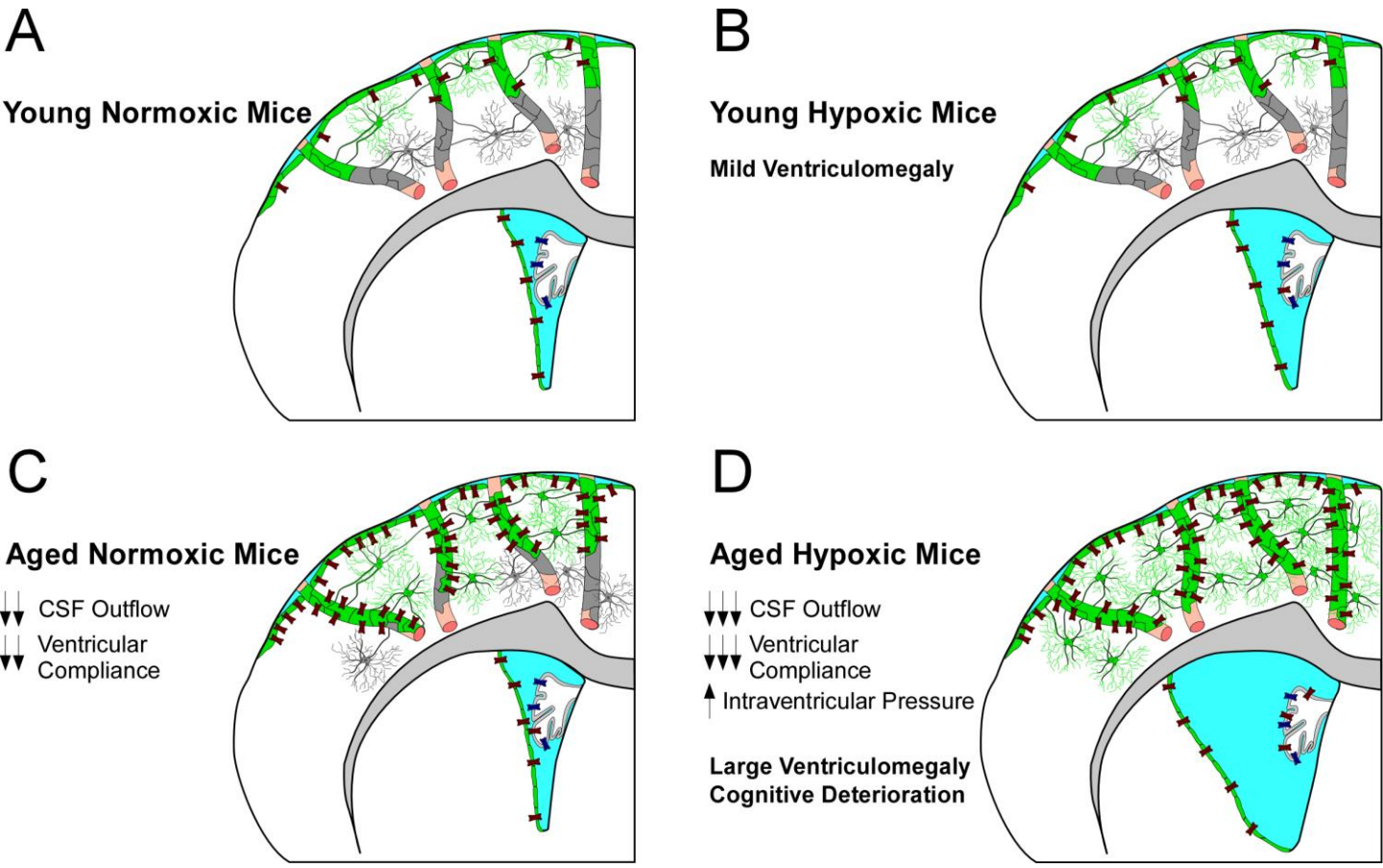
A
Young Normoxic Mice
B
Young Hypoxic Mice
Mild Ventriculomegaly
C
Aged Normoxic Mice
CSF Outflow
Ventricular Compliance
D
Aged Hypoxic Mice
CSF Outflow
Ventricular Compliance
Intraventricular Pressure
Large Ventriculomegaly
Cognitive Deterioration

Highlights

- Hypoxia and aging act synergistically to induce hydrocephalus in mice.
- AQP4, and not AQP1, is mainly responsible for the increase in CSF produced in hypoxia.
- AQP4 disorganization, lower CSF outflow and ventricular compliance in aged mice contribute to produce hydrocephalus.
- Chronic hypoxic aged mice appear as a good model to study chronic adult hydrocephalus.

Supplementary Material - 1

Gene	Primer forward	Primer reverse
AQP1	TTCACTTGGCCGCAATGA	CCAGCTGCAGAGTGCCAAT
AQP4	CCGTCTTCTACATCATTGCACAGT	GCGGTGAGGTTTCCATGAA
18S	AACGAGACTCTGGCATGCTAA	GCCACTTGTCCCTCTAAGAAGT

Supplementary Material - 2

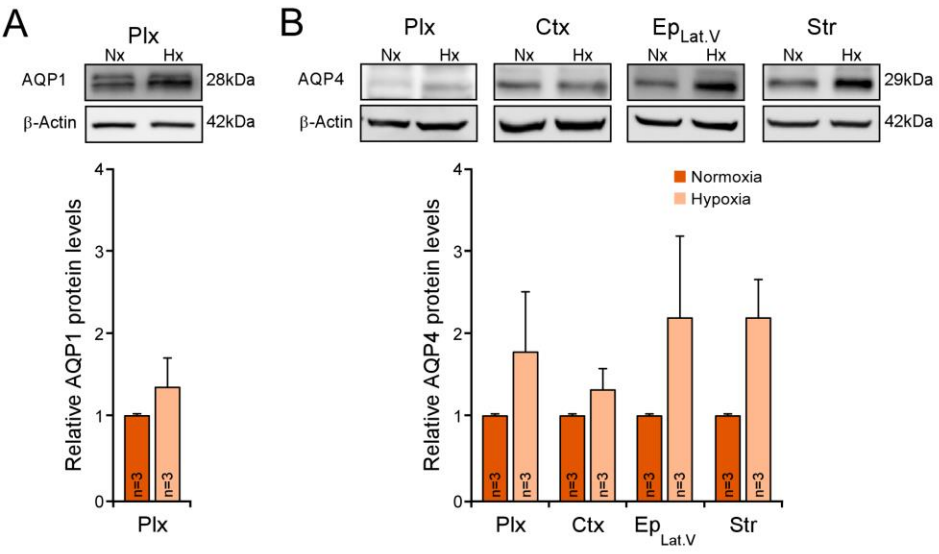

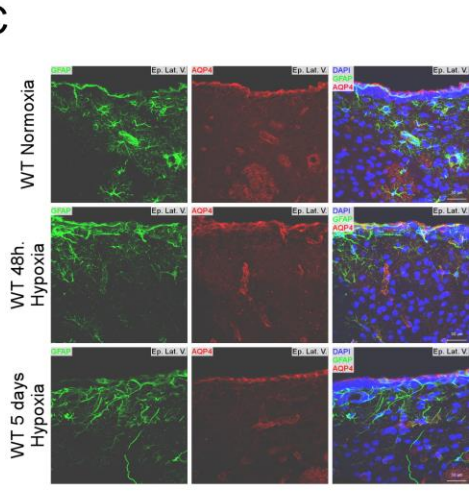

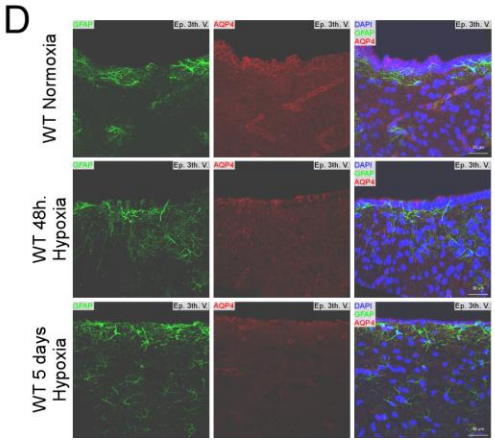

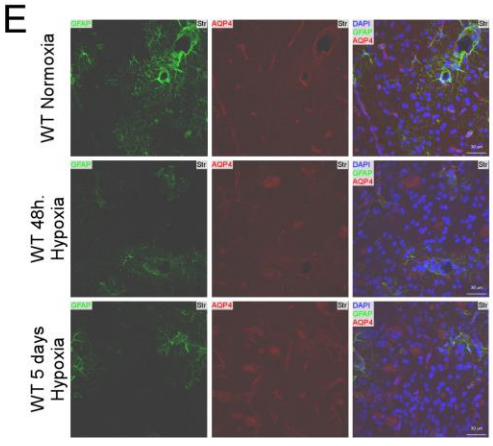

Supplementary Material – 3

A

	Young mice: systemic arterial pressure			
	n	Systolic blood pressure (mm Hg)	Diastolic blood pressure (mm Hg)	Mean blood pressure (mm Hg)
Normoxia				
wt	6	121,95 ± 3,90	52,74 ± 3,09	75,81 ± 3,29
AQP1$^{-/-}$	7	108,68 ± 7,41	44,75 ± 2,92	66,06 ± 4,19
AQP4$^{-/-}$	7	125,64 ± 2,16	47,20 ± 1,79	73,35 ± 1,78
Hypoxia				
wt	8	119,69 ± 2,80	51,17 ± 2,53	74,01 ± 2,17
AQP1$^{-/-}$	7	106,83 ± 4,80	52,37 ± 6,32	70,53 ± 5,73
AQP4$^{-/-}$	10	113,93 ± 6,00	47,07 ± 3,71	69,35 ± 4,30

B

	Aged mice: systemic arterial pressure			
	n	Systolic blood pressure (mm Hg)	Diastolic blood pressure (mm Hg)	Mean blood pressure (mm Hg)
Normoxia				
wt	7	119,57 ± 3,66	49,66 ± 2,25	72,96 ± 2,05
AQP1$^{-/-}$	4	109,29 ± 6,54	51,77 ± 6,66	70,94 ± 6,45
AQP4$^{-/-}$	7	123,21 ± 3,81	62,94 ± 4,54	83,03 ± 4,03
Hypoxia				
wt	10	107,54 ± 6,15	47,63 ± 2,08	67,60 ± 3,36
AQP1$^{-/-}$	4	110,57 ± 5,60	52,48 ± 4,62	71,84 ± 4,75
AQP4$^{-/-}$	7	117,07 ± 3,57	50,83 ± 2,36	72,91 ± 2,48

Supplementary Material - 4

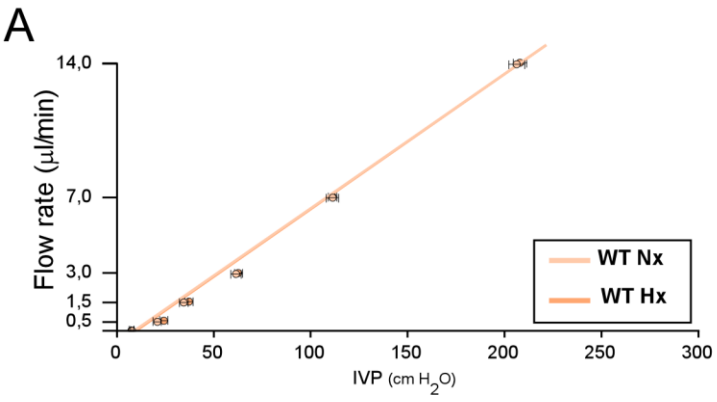

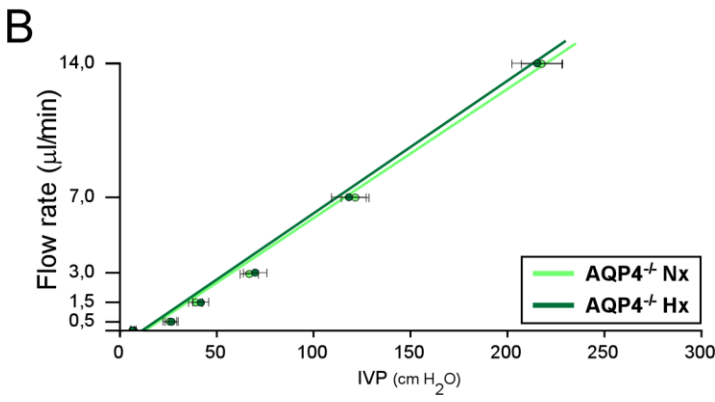

Supplementary Material - 5